Bone 93 (2016) 104–112

Contents lists available at ScienceDirect

Bone

journal homepage: www.elsevier.com/locate/bone

Full Length Article

# Reduced femoral bone mass in both diet-induced and genetic hyperlipidemia mice☆

Xiang Chen [a,1], Chunyu Wang [a,1], Kun Zhang [a], Ying Xie [a], Xiao Ji [a], Hui Huang [b], Xijie Yu [a,*]

[a] Laboratory of Endocrinology and Metabolism, Department of Endocrinology, West China Hospital, Sichuan University, 610041, People's Republic of China
[b] Department of Endocrinology, West China Hospital, Sichuan University, 610041, People's Republic of China

ARTICLE INFO

*Article history:*
Received 16 May 2016
Revised 24 August 2016
Accepted 19 September 2016
Available online 23 September 2016

*Keywords:*
Hyperlipidemia
Bone metabolism
Sphingosine-1-phosphate
*Peroxisome proliferator-activated receptor-γ*

ABSTRACT

Growing evidence argues for a relationship between lipid and bone metabolisms with inconsistent conclusions. Sphingosine-1-phosphate (S1P) has been recognized as a suitable candidate for possible link between lipid metabolism and bone metabolism. This study was designed to investigate the effects of hyperlipidemia on bone metabolism using diet-induced and genetic-induced hyperlipidemia animal models and to explore whether S1P is involved. Wild-type mice and low-density lipoprotein receptor gene deficient (*LDLR*$^{-/-}$) mice at age of 8 weeks were placed on either control diet or high-fat diet (HFD) for 12 weeks. Bone structural parameters were determined using microCT. Cross-linked type I collagen (CTx) and S1P levels in plasma were measured by ELISA methods. Bone marrow cells from wild type and *LDLR*$^{-/-}$ mice were induced to differentiate into osteoblasts, osteoclasts and adipocytes respectively. Gene expressions in distal femur metaphyses and cultured cells were studied by qRT-PCR. Moderate hypercholesterolemia was found in HFD-feeding mice; severe hypercholesterolemia and moderate hypertriglyceridemia were present in *LDLR*$^{-/-}$ mice. Femoral trabecular bone mass was reduced in both diet-induced and genetic hyperlipidemia mice. Mice feeding on HFD showed higher CTx levels, and mice with hyperlipidemia had elevated S1P levels. Correlation analysis found a positive correlation between CTx and S1P levels. Lower *Runx2* expression and higher *TRAP* expression were found in both diet-induced and genetic hyperlipidemia mice, indicating decreased osteoblastic functions and increased osteoclastic functions in these mice. Bone marrow cells from *LDLR*$^{-/-}$ mice also showed increased adipogenesis and inhibited osteogenesis accompanied by enhanced *PPARγ* expression. In conclusion, our study found decreased bone mass in both diet-induced and genetic hyperlipidemia mice.



## 1. Introduction

Previous studies found an increased risk of osteoporosis in subjects with atherosclerotic diseases or metabolic syndrome, suggesting an underlying link may mediate those chronic metabolic diseases. Hyperlipidemia, especially hypercholesterolemia, serving as the most prominent and well-established risk factor for atherosclerosis and a major component of metabolic syndrome, has been suggested to be the possible link. For example, higher risk of hip fracture was found in women after a diagnosis of a cardiovascular disease [1]. In postmenopausal women not taking hormone replacement therapy, total cholesterol (TC) and low density lipoprotein (LDL) levels have been found to be negatively associated with bone mineral density (BMD) at all measured sites [2] . In Japanese postmenopausal women, higher LDL-C levels were associated with increased risks for non-vertebral fractures [3]. Hypercholesterolemia mice also present an osteoporotic phenotype, including increased osteoclasts (OCs), reduced trabecular number and mechanical properties [4]. Statins, the first-line drugs for hypercholesterolemia, show beneficial influence of increasing BMD and reducing fracture risk in humans [5,6]. Statins regulate lipid metabolism exclusively through liver, where they inhibit cholesterol synthesis, leading to increased LDL uptake by the hepatocytes. Therefore, it seems likely that the beneficial effects of statins originate mainly from lipid-lowering, and not from direct effects on bone.

*Low-density lipoprotein receptor*-knockout (*LDLR*$^{-/-}$) mice, presenting with markedly increased serum TC, LDL-C levels and moderately elevated triglyceride (TG) levels as a result of impaired removal of

*Abbreviations:* BMD, bone mineral density; BMSC, Bone marrow stromal cell; Col1a1, collagen type 1 alpha-1; CTSK, cathepsin K; CTx, cross-linked type I collagen; HDL, high density lipoprotein; HFD, high-fat diet; LDL, low density lipoprotein; LDLR$^{-/-}$, Low-density lipoprotein receptor-knockout; LRP, low-density lipoprotein receptor-related protein; uCT, microCT; MMP9, matrix metallopeptidase 9; NFATc1, Nuclear factor-activated T cells c1; NHANES, National Health and Nutritional Examination Survey; OCN, osteocalcin; OPPG, osteoporosis-pseudoglioma syndrome; PPARγ, peroxisome proliferator-activated receptor-gamma; RANKL, the receptor activator of nuclear factor-kappa B ligand; Runx2, Runt-related transcription factor 2; S1P, sphingosine-1-phosphate; Tb·N, trabecular number; Tb·Sp, trabecular spacing; Tb·Th, trabecular thickness; TC, total cholesterol; TG, triglyceride; TRAP, resistant acid phosphatase; VF, visceral fat.

☆ Author disclosures: The authors declare that there are no conflicts of interest.

* Corresponding author at: Laboratory of Endocrinology and Metabolism, West China Hospital, Sichuan University, 610041, People's Republic of China.

[1] These authors contributed equally to this work.

http://dx.doi.org/10.1016/j.bone.2016.09.016
8756-3282/

cholesterol-rich lipoproteins from the plasma compartment, are widely used animal models for studying mechanism underlying hyperlipidemia related diseases such as atherosclerosis, type 2 diabetes and non-alcoholic steatohepatitis [7,8]. Soares et al. found smaller trabeculae, thinner spongy bone and impaired biomechanical properties in *LDLR*$^{-/-}$ mice, rendering these mice were more prone to fracture [9]. Low-density lipoprotein receptor-related protein 5 (LRP5) and LRP6, members of the LDLR family, are co-receptors of Wnt signaling pathway and are all involved in lipid as well as bone metabolism. Human carrying *LRP5* or *LRP6* mutations exhibit hypercholesterolemia and impaired glucose tolerance [10,11]. On the other hand, mice with either heterozygous or homozygous mutations in *LRP5* or heterozygous mutations in *LRP6* show limb defects and decreased BMD [12]. Homozygous loss-of-function mutations in *LRP5* lead to the autosomal recessive osteoporosis-pseudoglioma syndrome (OPPG) in human, presenting with severe osteoporosis and early onset blindness [13]. Furthermore, individuals carrying *LRP5* mutations showed lower BMD and higher prevalence of fractures accompanied by hypercholesterolemia [11]. The co-existence of deficient lipid and bone metabolism in carriers of mutant LDLR-related proteins further highlights their potential reciprocal interactions.

However, some studies got contrary results. Framingham Osteoporosis Study, enrolled 712 women and 450 men, found no long-term effects of cholesterol levels on BMD in women and men [14]. National Health and Nutritional Examination Survey (NHANES) III included 13,592 participants and also revealed no significant relationship between TC, LDL, or high density lipoprotein (HDL) levels and BMD after correcting for possible confounding factors [15]. Okayasu et al. reported increased bone mass in *LDLR*$^{-/-}$ mice due to impaired osteoclast formation as a result of defective osteoclastic cell-cell fusion [16]. Furthermore, previous studies reported different effects of hyperlipidemia on osteoblastic and osteoclastic functions [17–22]. The existence of a possible link between hypercholesterolemia and low BMD in most but not all studies indicates more investigations are needed to clarify their relationship.

Both bone and adipose tissue have been considered to have endocrine functions and are mutually regulated. On the one side, bone derived osteocalcin stimulates adiponectin secretion from adipose tissue, resulting in improved insulin sensitivity [23]. On the other side, adipose derived adipokines, such as leptin and adiponectin, show regulatory effects on bone. It is suggested that leptin inhibits bone formation through the central nervous system [24], while stimulates bone formation via the peripheral pathway [25]. Sphingosine-1-phosphate (S1P), a breakdown product of ceramide metabolism, is involved in the development of metabolic diseases including insulin resistance and type 2 diabetes [26–28]. Interestingly, S1P has been found to regulate bone homeostasis through mobilizing osteoclast precursors into bone marrow cavities, resulting in enhanced bone resorption [29,30]. Thus, S1P represents a suitable candidate for possible link between lipid metabolism and bone metabolism.

Therefore, in this study, we will investigate the effects of hyperlipidemia on bone metabolism and the possible mechanism using two hyperlipidemic animal models, and to explore whether S1P is involved.

## 2. Material and methods

### 2.1. Animals and intervention

All animal experiments were performed in accordance with the guidelines for the care and use of laboratory animals and were approved by the Institutional Animal Care and Use Committee at the West China Hospital, Sichuan University. All efforts were made to minimize animal suffering. 16 wild type mice (male) and 16 homozygous *LDLR* gene knockout mice (male) were obtained from the Jackson Laboratory (Bar Harbor, ME, USA). Both strains were on C57BL/6 J background and maintained in pathogen-free barrier conditions at animal facility of West China Hospital, Sichuan University. The animals were maintained in ventilated racks at a controlled temperature under a 12-h light/dark cycle, and free access to water and diet.

At age of 8 weeks, mice were randomly divided into four groups with 8 animals each: (1).WC group: wild-type mice, fed on chow diet; (2).WH group: wild-type mice, fed on HFD; (3). LC group: *LDLR*$^{-/-}$ mice, fed on chow diet; and (4). LH group: *LDLR*$^{-/-}$ mice, fed on HFD. Mice were placed on either a chow diet (64% carbohydrate, 10% fat and 26% protein) or a high-fat diet (28% carbohydrate, 60% fat and 12% protein) for 12 weeks. Both diets were bought from Trophic Animal Feed High-Tech Co., Ltd., (Nantong, Jiangsu, China). Mice were weighed weekly.

### 2.2. Plasma and tissue sampling

At the end of experiment, mice were euthanized with an intraperitoneal injection of sodium pentobarbital. Blood samples were collected and stored at −80 °C. Visceral fat (VF) (including epididymis fat and retroperitoneal fat) were weighed, immediately frozen in liquid nitrogen and stored at −80 °C. The right femora were immersed into 4% paraformaldehyde immediately and were used for detecting bone structural parameters. The left femora were immediately frozen in liquid nitrogen and stored at −80 °C for detecting mRNA expression levels of bone-related genes.

### 2.3. Blood chemistry

Plasma TG and TC levels were determined using COD-PAP method (Changchun Huili Biotech CO., LTD., Changchun, China). LDL-C was measured using direct method (Changchun Huili Biotech CO., LTD., Changchun, China). Fasting blood glucose was determined using Lifescan One touch glumeter (Johnson & Johnson, USA). Insulin levels were measured using an ultra-sensitive ELISA kit (Crystal Chem Inc., Illinois, USA). C-terminal telopeptide of type I collagen (CTx) and S1P were also measured by ELISA methods (Wuhan USCN Business co., Ltd., Wuhan, China; MyBioSource, San Diego, California, USA).

### 2.4. MicroCT 80 for bone structural parameters

Bone structural parameters of *LDLR*$^{-/-}$ and wild-type femora were measured using microcomputed tomography (μCT) (MicroCT80, Scanco Medical AG, Bassersdorf, Switzerland), as previously described [31,32]. Briefly, femurs were scanned for microarchitecture in the metaphyseal region of the distal femur at the energy level of 55 keV, and intensity of 177 μA. The distal trabecular scan started about 0.6 mm proximal to the growth plate and extended proximally 1.5 mm. 100 contiguous slices were used for analysis [33]. This instrument provides high-resolution data for trabecular and cortical bone volume, as well as trabecular number (Tb·N), trabecular thickness (Tb·Th), and trabecular separation (Tb·Sp).

### 2.5. Real-time qRT-PCR for bone-related gene expression

Femur distal metaphyses were resected and chopped finely with a scalpel as previously described [32]. Total RNA was extracted using Trizol reagent according to the manufacturer's protocol (Invitrogen, Frederick, USA). 1 μg RNA was reversely transcribed into cDNA with PrimeScriptR RT reagent kit (TaKaRa Biotechnology Co., Ltd., Dalian, China). Following reverse transcription, the cDNA (2 μl) was amplified and quantified (Bio—Rad laboratories, Inc., California, USA). The sequence of oligonucleotide primers was listed in Table 1. Each RNA sample was analyzed in triplicate. GAPDH was used as an endogenous control. The relative mRNA expression levels were normalized to the GAPDH in the same sample and analyzed with the $2^{-\Delta\Delta CT}$ method as our previous report [34]. Total RNA was also extracted from visceral fat to study gene expression of *leptin* in the similar way.

**Table 1**
Oligonucleotide primers for cDNA amplification.

| Oligonucleotide | Sequence (5′–3′) | Product length | Corresponding cDNA sequence |
|---|---|---|---|
| *c-Fos* forward primer | AGAGCGGGAATGGTGAAGAC | 194 | 461–480 |
| *c-Fos* reverse primer | AGTTGATCTGTCTCCGCTTGG | | 654–634 |
| *Col1a1* forward primer | GCGAAGGCAACAGTCGCT | 101 | 4166–4183 |
| *Col1a1* reverse primer | CTTGGTGGTTTTGTATTCGATGAC | | 4266–4243 |
| *CTSK* forward primer | GAAGAAGACTCACCAGAAGCAG TCCAGGTTATGGGCAGAGATT | 102 | 677–698 |
| *CTSK* reverse primer | | | 778–698 |
| *GAPDH* forward primer | TGCACCACCAACTGCTTAG | 177 | 520–538 |
| *GAPDH* reverse primer | GGATGCAGGGATGATGTTC | | 696–678 |
| *Leptin* forward primer | GGAAAATGTGCTGGAGACCC | 158 | 55–74 |
| *Leptin* reverse primer | TACCGACTGCGTGTGTGAAAT | | 212–192 |
| *MMP9* forward primer | CTGGACAGCCAGACACTAAAG CTCGCGGCAAGTCTTCAGAG | 145 | 297–317 |
| *MMP9* reverse primer | | | 441–422 |
| *NFATc1*forward primer | GACATGACGGGGCTGGAG TAACTGTAGTGTTCTGCGGC | 101 | 53–70 |
| *NFATc1*reverse primer | | | 153–134 |
| *OCN* forward primer | CTCACAGATGCCAAGCCC CCAAGGTAGCGCCGGAGTCT | 98 | 109–126 |
| *OCN* reverse primer | | | 206–187 |
| *PPARγ* forward primer | TTCGCTGATGCACTGCCTAT | 271 | 94–113 |
| *PPARγ* reverse primer | TGATCGCACTTTGGTATTCTTGG | | 364–342 |
| *Runx2* forward primer | GTGGTAGGCAGTCCCACTTT | 272 | 47–66 |
| *Runx2* reverse primer | GAGCACTCACTGACTCGGTT | | 318–299 |
| *TRAP* forward primer | CAGCAGCTCCCTAGAAGATGG | 284 | 118–138 |
| *TRAP* reverse primer | CTGGAACCTCTTGTCGCTGG | | 401–382 |

*Col1a1*: *collagen type I alpha 1*; *CTSK*: *cathepsin K*; *MMP9*: *matrix metallopeptidase 9*; *NFATc1*: *Nuclear factor of activated T cells, cytoplasmic 1*; *OCN*: *osteocalcin*; *PPARγ*, *peroxisome proliferator-activated receptor gamma*; *Runx2*, *runt-related transcription factor 2*; *TRAP*: *tartrate-resistant acid phosphatase.*

### 2.6. Comparison of osteoblast and osteoclast differentiation between WT and $LDLR^{-/-}$ mice in vitro

#### 2.6.1. Bone marrow stromal cell (BMSC) cultures

Femur and tibia from WT and $LDLR^{-/-}$ mice were used for BMSC cultures as previously described [32]. Bone marrow cells were flushed out with a 3 $cm^3$ syringe and 25G needle. Cells were collected, counted and plated on 24-well plates at a density of $1 \times 10^6$/well at 37 °C in α-MEM, supplemented with 10% FBS, 1% penicillin/streptomycin. The day of plating was counted as day 0. Plated cells became confluent around days 5–6 and total RNA was extracted to measure *peroxisome proliferator-activated receptor-γ* (*PPARγ*) expression.

#### 2.6.2. Osteoblast and adipocyte differentiation

At day 7, the culture medium was changed to differentiation medium consisting of regular medium, 50 μg/ml ascorbic acid, and 10 mM beta-glycerophosphate for osteogenic differentiation. For adipogenic differentiation, culture medium was changed to adipogenic medium containing StemPro® Adipogenesis Differentiation Kit from Gibco (Thermo Fisher Scientific Inc., U.S.). Alkaline phosphatase (ALP) staining with a kit from Sigma (sigma, U.S.) and Oil red O staining were performed to determine osteogenic and adipogenic differentiation respectively. After osteoblast induction for 7 days, expression levels of osteoblast-related genes including *Runt-related transcription factor 2* (*Runx2*), *collagen type 1 alpha-1* (*Col1a1*) and *osteocalcin* (*OCN*) were determined as stated before.

#### 2.6.3. Osteoclast differentiation

Bone marrow cells were collected as above and plated on 24-well plates at a density of $1 \times 10^6$/well at 37 °C in α-MEM, supplemented with 10% FBS, 1% penicillin/streptomycin, 25 ng/ml of human macrophage-colony stimulating factor (M-CSF) (R&D Systems, U.S.) and 30 ng/ml of human soluble receptor activator of NF-κB ligand (RANKL) (R&D Systems, U.S.). Medium was changed every 3 days. 7 days later, resistant acid phosphatase (TRAP) staining with a kit from Sigma (sigma, U.S.) was performed to determine osteoclast formation. TRAP-positive cells containing 3 or more nuclei were counted as osteoclast. Osteoclast numbers of each well and nuclear numbers of each osteoclast were calculated from 6 wells/group using bright-field light microscopy (Zeiss, Germany). Expression levels of osteoclast-related genes including *nuclear factor-activated T cells c1* (*NFATc1*), *c-Fos*, *TRAP*, *cathepsin K* (*CTSK*) and *matrix metallopeptidase 9* (*MMP9*) were determined as stated before.

### 2.7. Statistical analyses

Data were presented as means ± SDs and were analyzed using SPSS 16.0 software. The comparison of metabolic variables, bone structural parameters and relative gene expression levels among WC, WH, LC and LH groups were analyzed using two-way factorial ANOVA to test the main effects of different genotypes and diets. The comparison of gene expression levels between WT mice and $LDLR^{-/-}$ mice were analyzed using independent- sample *t*-test. Correlation analysis was performed using pearson correlation coefficient. The statistical significance was set at $P < 0.05$ (two tails).

## 3. Results

### 3.1. Metabolic parameters

No significant differences in body weight were found among the four groups, whereas a significant increase in VF/body weight ratio was observed in group LH when compared to groups WC, WH and LC (Fig. 1A, B). As expected, plasma TC levels were different among the four groups in the following order: WC < WH < LC < LH (Fig. 1C). No differences in plasma TG and LDL-C were observed between groups WC and WH. However, $LDLR^{-/-}$ mice showed higher TG and LDL-C levels when compared with WT mice on the same diet; the TG and LDL-C levels were further increased upon HFD feeding in group LH compared to group LC (Fig. 1D, E). Plasma insulin and blood glucose levels were comparable among groups (data not shown). Mice in groups WH and LH showed higher plasma CTx levels (Fig. 1F). Higher S1P levels were found in mice with hyperlipidemia (Fig. 1G.) Fig.1H showed a positive correlation between plasma CTx and S1P levels ($r = 0.514$, $p = 0.006$).

Factorial ANOVA analysis showed significant main effects of genotypes on plasma TC, TG, LDL-C and S1P levels, significant main effects of diets on TC levels, VF/body weight ratio, CTx and S1P levels. Significant genotype-by-diet interactions were noted for plasma S1P levels (Table 2).

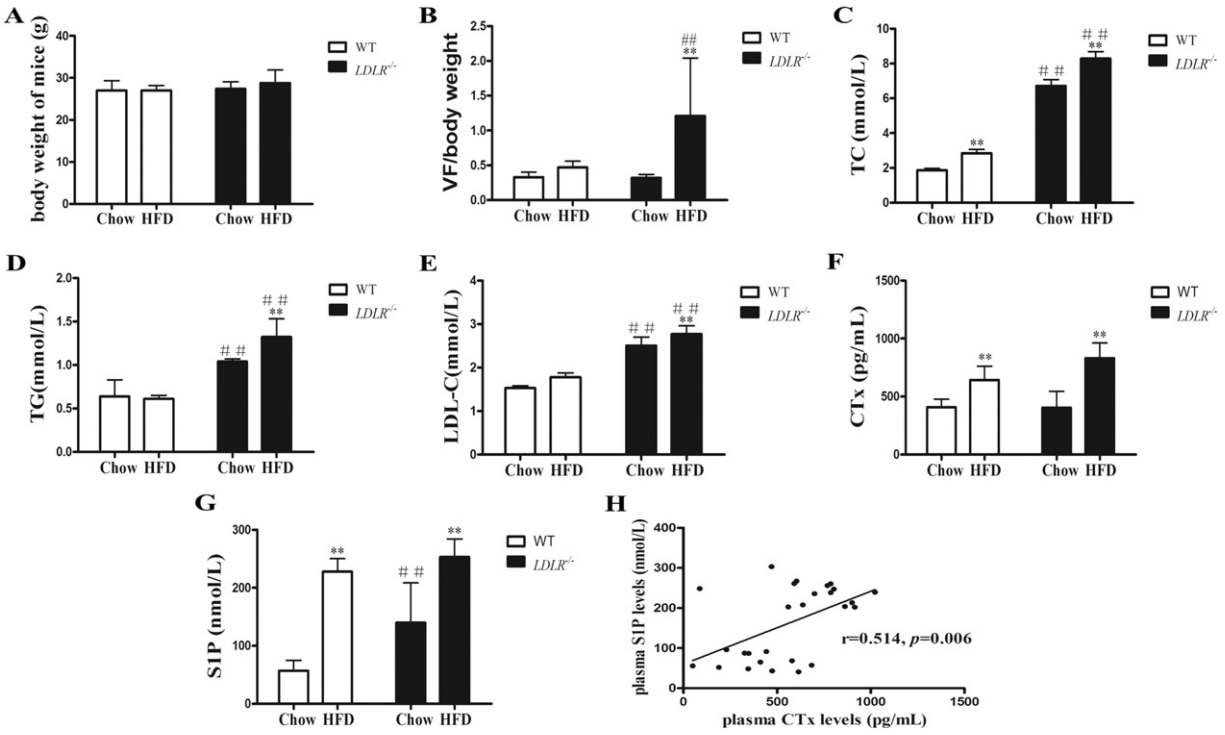


**Fig. 1.** Comparison of metabolic parameters among groups. A. Body weights of mice. B. VF/body weight. C. TC levels were different among groups in the following order: WC < WH < LC < LH. D. TG levels were higher in $LDLR^{-/-}$ mice. E. LDL-C levels were higher in $LDLR^{-/-}$ mice. F. CTx levels were higher in HFD-feeding mice. G. Hyperlipidemia mice present with higher S1P levels. H. Plasma S1P levels were positively associated with CTx levels ($r = 0.514$, $p = 0.006$) (*$P < 0.05$, **$P < 0.01$, compared to the same genotype, #P < 0.05, ##P < 0.01, compared to the same diet, $n = 8$).

**Table 2**
Two-way factorial ANOVA analyses of metabolic variables, bone structural parameters and relative gene expression levels among groups WC, WH, LC and LH.

| Variables | *P* | Main effect of genotype | Main effect of diet | Genotype by diet interaction |
|---|---|---|---|---|
| Body weight (g) | 0.54 | 0.28 | 0.49 | 0.49 |
| VF/body weight | 0.01 | 0.08 | 0.02 | 0.06 |
| TC (mmol/L) | 0.01 | 0.01 | 0.00 | 0.29 |
| TG (mmol/L) | 0.01 | 0.01 | 0.38 | 0.29 |
| LDL-C (mmol/L) | 0.01 | 0.01 | 0.07 | 0.95 |
| Insulin (pmol/L) | 0.90 | 0.74 | 0.59 | 0.74 |
| Blood glucose (mmol/L) | 0.28 | 0.29 | 0.51 | 0.15 |
| S1P (nmol/L) | 0.01 | 0.01 | 0.01 | 0.04 |
| CTx (pg/mL) | 0.01 | 0.23 | 0.01 | 0.25 |
| Tb. BV/TV | 0.01 | 0.04 | 0.00 | 0.01 |
| Tb·Th (mm) | 0.19 | 0.68 | 0.10 | 0.18 |
| Tb·N (1/mm) | 0.51 | 0.38 | 0.70 | 0.23 |
| Tb·Sp (mm) | 0.34 | 0.17 | 0.56 | 0.21 |
| Cort.BV/TV | 0.05 | 0.18 | 0.03 | 0.42 |
| *Runx2* expression levels | 0.03 | 0.02 | 0.04 | 0.67 |
| *Col1a1* expression levels | 0.01 | 0.01 | 0.55 | 0.38 |
| *TRAP* expression levels | 0.049 | 0.03 | 0.94 | 0.08 |
| *CTSK* expression levels | 0.01 | 0.01 | 0.30 | 0.29 |
| *MMP9* expression levels | 0.01 | 0.01 | 0.07 | 0.75 |
| Leptin expression levels | 0.04 | 0.02 | 0.33 | 0.18 |

VF, visceral fat; TC, total cholesterol; TG, triglyceride; LDL-C, low density lipoprotein- cholesterol; S1P, sphingosine-1-phosphate; CTx, cross-linked type I collagen; Tb. BV/TV, trabecular bone volume/total volume; Tb·Th, trabecular thickness; Tb·N, trabecular number; Tb·Sp, trabecular spacing; Cort.BV/TV, cortical bone volume/total volume; *Runx2*, *runt-related transcription factor 2*; *Col1a1*: *collagen type I alpha 1*; *TRAP*: *tartrate-resistant acid phosphatase*; *CTSK*: *cathepsin K*; *MMP9*: *matrix metallopeptidase 9.*

### 3.2. Bone mass and structure

μCT was used to evaluate effects of genotype and diet on microstructural properties of femora. In the comparison of the trabecular bone mass of femora, the bone volume to tissue volume ratio (BV/TV) was significant lower in groups WH and LH compared to groups WC and LC respectively, and group LC also showed lower BV/TV compared with group WC (Fig. 2A). No differences were found in Tb·Th, Tb·N and Tb·Sp among the four groups (Fig. 2B, C, D). When comparing cortical bone mass of femora, we observed a tendency to decrease in cortical BV/TV in group LH when compared to groups WH and LC ($p = 0.05$, Table 2, Fig. 2E). Two-factor ANOVA analysis showed significant main effects of genotypes, diets and genotype-by-diet interactions on trabecular bone mass of femora (Table 2). Our results also showed significant main effects of diets on cortical bone mass of femora (Table 2).

### 3.3. mRNA expression of bone and adipose genes

*Runx2* is a key transcription factor for the commitment of pluripotent mesenchymal cells into the osteoblastic lineage [35]. For the same genotype comparison, we found a significantly lower expression of *Runx2* in group WH compared to group WC; for the same diet comparison, $LDLR^{-/-}$ mice showed lower *Runx2* expression on each diet (Fig.3 A). For the same diet comparison, mice in group LH showed lower *Col1a1* expression compared with group WH (Fig.3 B). Two-way ANOVA analysis showed significant main effects of genotypes on expression levels of *Runx2* and *Col1a1,* significant main effects of diets on expression levels of *Runx2*. No significant genotype-by-diet interactions were noted (Table 2).

M-CSF an RANKL are two key factors involved in osteoclast differentiation [36,37]. The binding of RANKL to its receptor RANK on osteoclast precursors will lead to the expression of various osteoclast genes including *TRAP*, *CTSK* and *MMP9* [36,37]. Thus, the expression levels of *TRAP, CTSK* and *MMP9* reflect osteoclast numbers and activities to a certain

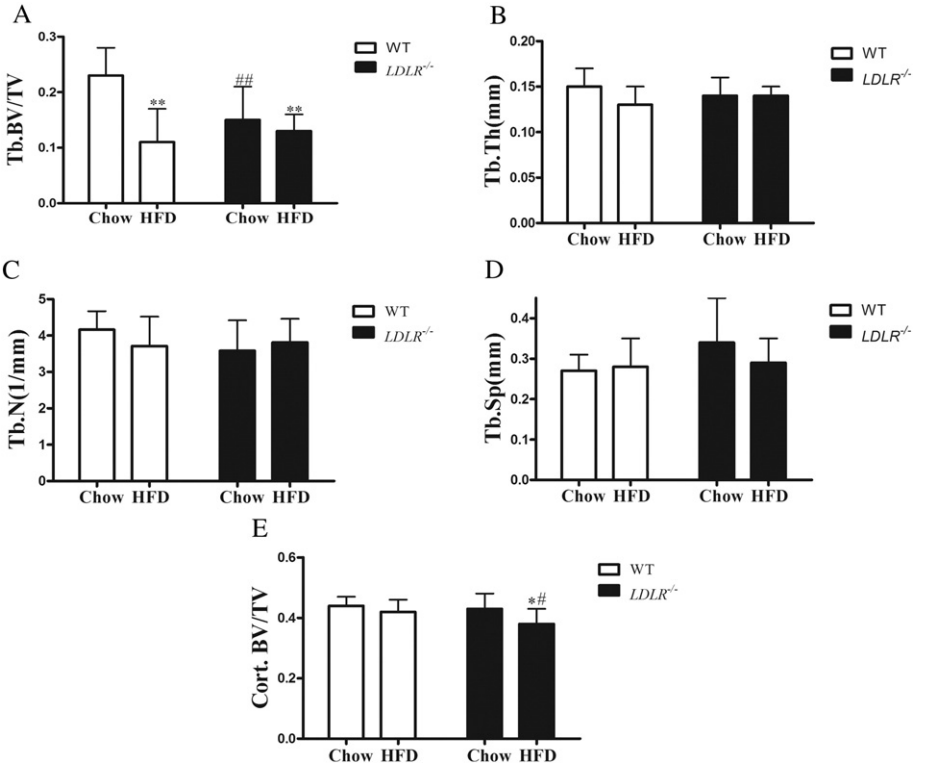


**Fig. 2.** Decreased bone mass in diet-induced and genetic hyperlipidemia mice. A. Trabecular bone volume (Tb. BV/TV). B. Trabecular bone thickness (Tb·Th). C. Trabecular bone number (Tb. N). D. Trabecular separation (Tb·Sp). E. Cortical bone volume (Cort. BV/TV). ($^{*}P < 0.05$, $^{**}P < 0.01$, compared to the same genotype, $^{\#}P < 0.05$, $^{\#\#}P < 0.01$, compared to the same diet, $n = 8$).

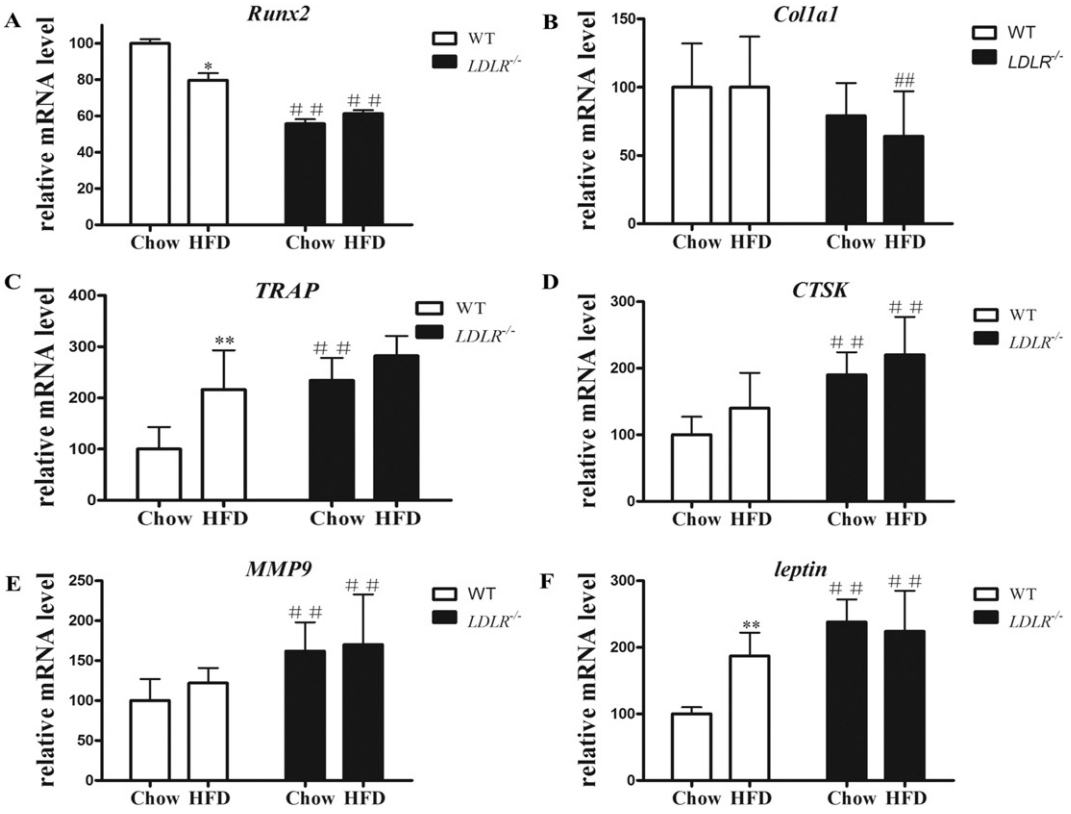


**Fig. 3.** Relative mRNA expression levels of bone- and adipose-related genes. A. *Runx2* expression was decreased in groups WH, LC and LH. B. Mice in group LH showed lower *Col1a1* expression compared with group WH. C. The expression levels of *TRAP* in group WH were higher compared to group WC; mice in group LC also had higher *TRAP* expression compared to group WC. D and E. $LDLR^{-/-}$ mice showed higher *CTSK* and *MMP9* expression compared to WT mice on the same diet. F. Higher *leptin* expression levels in groups WH, LC and LH. ($^{*}P < 0.05$, $^{**}P < 0.01$, compared to the same genotype, $^{\#}P < 0.05$, $^{\#\#}P < 0.01$, compared to the same diet, $n = 8$).

extent. The expression levels of *TRAP* in group WH were higher compared to group WC; mice in group LC also had higher *TRAP* expression compared to group WC (Fig. 3C). For the same diet comparison, *LDLR*$^{-/-}$ mice showed higher *CTSK* and *MMP9* expression on each diet when compared to WT mice (Fig.3D, E). Two-way ANOVA analysis showed significant main effects of genotypes on expression levels of *TRAP, CTSK* and *MMP9*. No significant genotype-by-diet interactions were noted (Table 2). The above data suggested that hyperlipidemia mice showed inhibited bone formation and enhanced osteoclast formation, these phenotypes more pronounced in *LDLR*$^{-/-}$ mice.

The relative expression levels of *leptin* in visceral fat in group WH were higher than those in group WC; *LDLR*$^{-/-}$ mice showed higher *leptin* expression levels compared to WT mice on the same diet (Fig. 3F). Factorial ANOVA showed significant main effects due to genotypes on expression level of *leptin* (Table 2).

### *3.4. Comparison of osteoblast and osteoclast differentiation in vitro between WT and LDLR*$^{-/-}$ *mice*

BMSCs cultures showed reduced osteogenic differentiation and enhanced adipogenic differentiation in *LDLR*$^{-/-}$ mice compared to that in WT mice (Fig. 4). BMSCs differentiation is under the regulation of *PPARγ* and *Runx2*. Real time PCR showed higher *PPARγ* expression levels in BMSCs of *LDLR*$^{-/-}$ mice (Fig. 5). Osteoblast-related gene analysis showed lower *Runx2*, *Col1a1* and *OCN* expression levels in *LDLR*$^{-/-}$ mice (Fig.5). The above data suggested reduced osteoblastogenesis in *LDLR*$^{-/-}$ mice.

Osteoclast cultures in vitro showed increased osteoclast numbers and more average nuclear numbers/ osteoclast in *LDLR*$^{-/-}$ mice (Fig.4). *NFATc1* is the key regulator of osteoclast differentiation. Our data showed increased *NFATc1* expression in *LDLR*$^{-/-}$ mice (Fig. 5). Other osteoclast-related gene analysis showed higher *c-Fos*, *TRAP*, *CTSK* and *MMP9* expression in *LDLR*$^{-/-}$ mice (Fig. 5). These data indicated enhanced osteoclast formation and functions in *LDLR*$^{-/-}$ mice.

## 4. Discussion

The present study demonstrated different lipid profiles in diet-induced and genetic-induced hyperlipidemia animal models. *LDLR*$^{-/-}$ mice showed moderate hypertriglycemia and severe hypercholesterolemia, and the hypercholesterolemia was further aggravated upon high-fat feeding. While in wild-type mice, only moderate hypercholesterolemia was induced by high-fat feeding. Accordingly, the trabecular bone mass was reduced in mice with hyperlipidemia, including WT mice on high-fat diet and *LDLR*$^{-/-}$ mice on either diet. Notably, the combination of diet-induced and genetic hyperlipidemia caused more pronounced bone loss than either condition alone, since genotype-by-diet interactions on trabecular bone mass were found in factorial ANOVA analysis ($p = 0.01$, Table 2) and both the trabecular and cortical bone mass were reduced in LH mice. In general, trabecular bone is more responsive to diet, drug treatments, or aging than cortical bone does because trabecular bone is more actively remodeled [17].

Bone remodeling is a dynamic process for the whole lifetime, regulated by the elaborate equilibrium between bone formation and bone resorption. In physiological state, bone formation and bone resorption are subtle and well coupled processes. Most but not all previous studies found reduced bone mass in HFD feeding mice, especially cancellous bone. However, regarding the mechanism, related researches reported different effects of HFD feeding on osteoblastic or osteoclastic functions. Cao et al. found reduced cancellous bone mass in HFD feeding mice, and those obese mice showed increased osteoblastic function (possibly due to higher body weight) and enhanced osteoclastic resorption [17]. Shu et al. also found elevated osteoblast and osteoclast numbers in bone marrow cells from HFD-feeding juvenile mice with less bone mass [19]. However, in another study, Cao et al. found decreased femoral trabecular bone mass in obese mice, possibly due to impaired osteoblastic function (reflected by reduced osteocalcin levels in serum) and enhanced osteoclastic function [18]. Patsch et al. found short-term and extended high-fat diet feeding significantly increased serum CTx levels

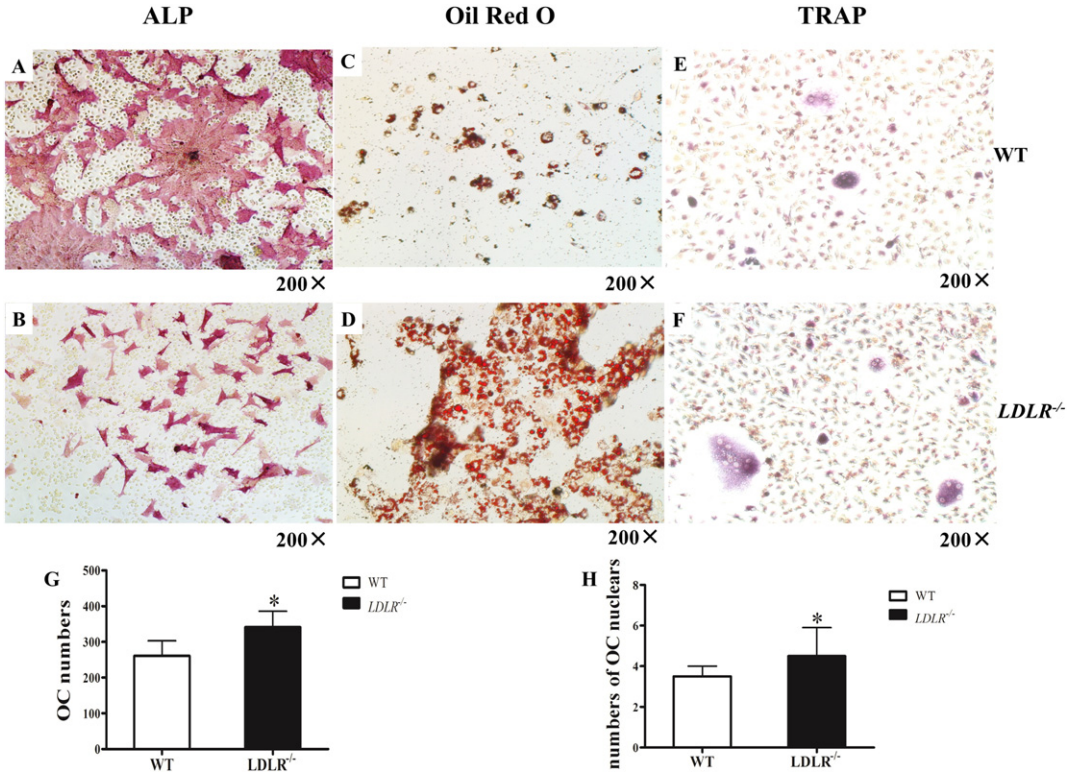


**Fig. 4.** Different ability of osteoblastogenesis, adipocyteogenesis and osteoclastogenesis between WT and *LDLR*$^{-/-}$ mice. A and B. ALP staining showed reduced osteoblast differentiation in *LDLR*$^{-/-}$ mice. C and D. Oil Red O staining demonstrated enhanced adipocyte differentiation in *LDLR*$^{-/-}$ mice. E and F. TRAP staining showed increased osteoclast differentiation in *LDLR*$^{-/-}$ mice. G and H. Both of osteoclast numbers per well and average nuclear numbers per osteoclast were increased in *LDLR*$^{-/-}$ mice. OC, osteoclast. (*$P < 0.05$, compared to WT, $n = 6$).

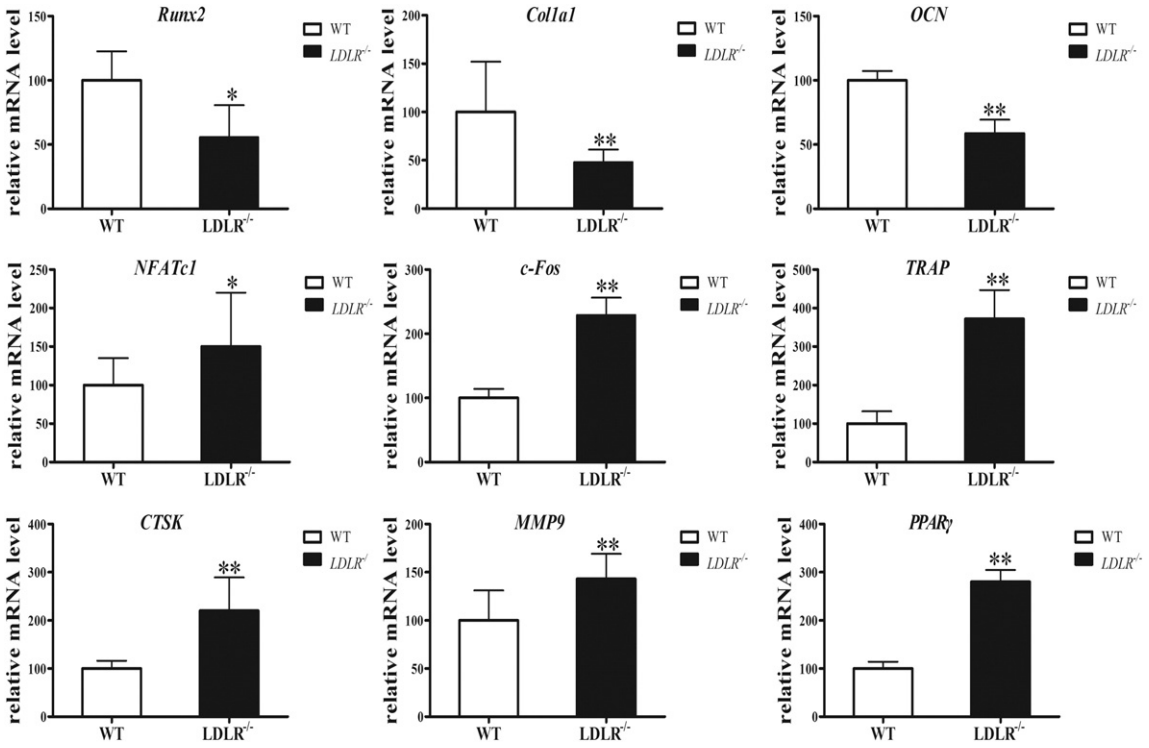


**Fig. 5.** Relative mRNA expression levels by qRT-PCR. Osteoblast-related genes, including *Runx2*, *Col1a1* and *osteocalcin*, were lower in $LDLR^{-/-}$ mice. Osteoclast-related genes, including *NFATc1*, *c-Fos*, *TRAP*, *CTSK* and *MMP9* were higher in $LDLR^{-/-}$ mice. Expression levels of *PPARγ* of bone marrow cells from $LDLR^{-/-}$ mice were also higher. ($^{*}P < 0.05$, $^{**}P < 0.01$, compared to WT, $n = 8$).

and caused similar bone loss with no obvious effects on serum osteocalcin levels, indicating high-fat diet–induced bone loss mainly originates from resorptive changes in trabecular architecture. Different results may be related to different animal models, different interventions, in particular the use of different methods to evaluate the function of osteoblasts and osteoclasts.

In this study, WH mice showed inhibited *Runx2* and elevated *TRAP* expression in femur distal metaphyses, as well as increased plasma CTx levels compared with WC mice, indicating decreased osteoblastic functions and enhanced osteoclastic functions induced by HFD feeding. On the other hand, compared with WT mice, $LDLR^{-/-}$ mice presented with lower *Runx2* and higher *TRAP*, *CTSK* and *MMP9* expression in femur distal metaphyses; in vitro cell cultures also demonstrated inhibited osteoblast differentiation and enhanced osteoclast differentiation of bone marrow cells from $LDLR^{-/-}$ mice. These data suggest that HFD-induced and *LDLR* knockout –induced hyperlipidemia may

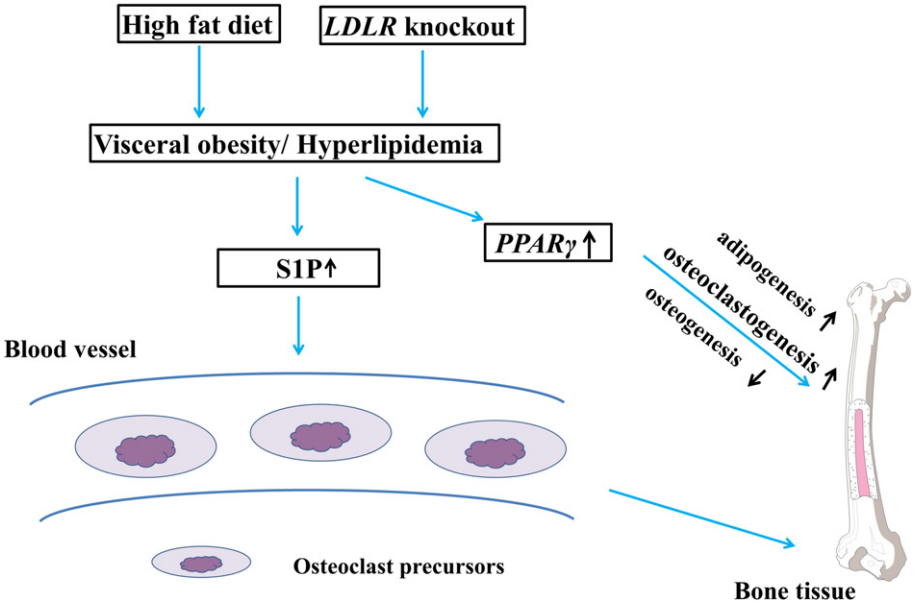


**Fig. 6.** *PPARγ* and S1P are possibly involved in the bone loss induced by hyperlipidemia. Diet-induced and genetic-induced hyperlipidemia and obesity increase plasma S1P levels, which mobilizes more osteoclast precursors into bone marrow cavities, resulting in enhanced bone resorption. On the other hand, *PPARγ* expression is increased in bone marrow cells from mice with hyperlipidemia, which stimulates adipogenesis and osteoclastogenesis while inhibits osteogenesis.

decrease bone formation and enhance bone resorption. Consistent with the study by Pirih et al., we found that these phenotypes were more obvious in *LDLR*$^{-/-}$ mice [22]. Another study also showed greater osteoclastic potential of bone marrow cells ex vivo from *LDLR*$^{-/-}$ mice versus wild type mice [38].

The mechanism underlying hyperlipidemia induced abnormal bone metabolism is very complex. In our study, inhibited osteoblastic functions in hyperlipidemia mice may be related to the changes in Runx2 and *PPARγ*. BMSCs are pleiotropic cells, capable of differentiating into osteoblasts, adipocytes and chondrocytes. The differentiation of BMSCs into osteoblasts and adipocytes are negatively related, under the regulation of *Runx2* and *PPARγ* [39–41]. *PPARγ* is predominately expressed in adipose tissue, acting as a master switch in controlling adipocyte proliferation and differentiation [42]. *PPARγ* also stimulates adipogenesis and inhibits osteogenesis, and vice versa of Runx2 [39,40]. Our study found significantly increased *PPARγ* expression while decreased Runx2 in *LDLR*$^{-/-}$ mice, which may impair osteoblast differentiation and result in decreased bone formation.

Except for its role in BMSCs differentiation, *PPARγ* also plays a role in regulating osteoclastogenesis [43]. Wan et al. demonstrated that *Tie2Cre/flox* mouse, in which *PPARγ* is conditionally deleted in osteoclasts but not in osteoblasts, developed osteopetrosis as a result of reduced osteoclast differentiation [44]. Mechanically, *PPARγ* directly regulates *c-Fos* expression, which is an essential mediator of osteoclastogenesis [44]. Our study also showed increased *PPARγ* and *c-Fos* expression in bone marrow cells from *LDLR*$^{-/-}$ mice. Furthermore, another study suggested that mouse bone marrow microenvironment was altered by HFD feeding with increased osteoclast precursor as well as increased expression of osteoclastogenic regulators including *RANKL* and *PPARγ* [19], further indicating *PPARγ* may play a key role in regulating the differentiation of osteoclasts in bone marrow cells. Therefore, PPARγ agonists are not recommended in diabetic patients with osteoporosis [45].

In the present study, we also investigated whether S1P is involved in the abnormal bone metabolism caused by hyperlipidemia. Abnormal sphingolipid metabolism is closely associated with obesity and HFD feeding. HFD enhances de novo sphingolipid synthesis and elevates S1P levels in several tissues, such as liver, skeletal muscle, adipose tissue, and cardiovascular tissues [46]. Accordingly, serum S1P levels were elevated in *ob/ob* mice and obese humans [26,27]. In cultured adipocytes, S1P stimulated gene expression of *plasminogen activator inhibitor-1*, *tumor necrosis factor (TNF)-α*, *monocyte chemoattractant protein-1* and *interleukin-6* (*IL-6*) [27]. Proinflammatory cytokines TNF-α and IL-6 directly or indirectly regulate osteoclastogenesis [47]. More importantly, S1P could mobilize osteoclast precursors into bone marrow cavities, resulting in enhanced bone resorption [29]. Accordingly, plasma S1P levels were inversely correlated with bone mineral density, whereas positively correlated with bone resorption markers in postmenopausal women [48]. Our study showed higher plasma S1P levels in hyperlipidemia mice, including WT on HFD and *LDLR*$^{-/-}$ mice on either diet. A positive correlation was also observed between plasma CTx and S1P levels, indicating S1P may be involved in the enhanced bone resorption induced by hyperlipidemia (Fig. 6). The mechanism deserves further investigation. To the best of our knowledge, this is the first study which has investigated the effects of *LDLR* knockout on the abilities of bone marrow cells differentiating into osteoblasts, osteoclasts and adipocytes. We are also the first to report S1P may be involved in the hyperlipidemia induced abnormal bone metabolism.

Previous studies suggest that adipose tissue and bone are mutually regulated [49–51]. Adipocytes and osteoblastogenitors coexist in bone marrow cavity. Adipocyte-derived adipokines, such as leptin and adiponectin, show ability to regulate osteoblast and osteoclast functions [49,52]. Our study showed higher *leptin* expression in visceral adipose tissue in mice with hyperlipidemia, consistent with a previous study [18]. It was suggested that elevated serum leptin may inhibit bone formation [18,53].

## 5. Conclusions

In conclusion, we demonstrated that hyperlipidemia reduced bone formation and enhanced bone resorption, resulting in lower femoral bone mass in mice. We also found higher plasma S1P levels in hyperlipidemia mice and a positive correlation between plasma CTx and S1P levels, indicating S1P may be involved in hyperlipidemia induced abnormal bone metabolism.

## Funding

This work was supported by grants from the National Natural Science Foundation of China (Nos. 81572639, 81370969 to X Yu), the Ministry of Education of the People's Republic of China (No. 20130181110066 to X Yu), and the Chengdu Bureau of Science and Technology (No. 2014-HM01-00382-SF to X Yu).

## References

[1] U. Sennerby, B. Farahmand, A. Ahlbom, S. Ljunghall, K. Michaelsson, Cardiovascular diseases and future risk of hip fracture in women, Osteoporos. Int. 18 (2007) 1355–1362.
[2] J. Makovey, J.S. Chen, C. Hayward, F.M. Williams, P.N. Sambrook, Association between serum cholesterol and bone mineral density, Bone 44 (2009) 208–213.
[3] M. Yamauchi, T. Yamaguchi, K. Nawata, K. Tanaka, S. Takaoka, T. Sugimoto, Increased low-density lipoprotein cholesterol level is associated with non-vertebral fractures in postmenopausal women, Endocrine 48 (2015) 279–286.
[4] K. Pelton, J. Krieder, D. Joiner, M.R. Freeman, S.A. Goldstein, K.R. Solomon, Hypercholesterolemia promotes an osteoporotic phenotype, Am. J. Pathol. 181 (2012) 928–936.
[5] K.A. Chan, S.E. Andrade, M. Boles, D.S. Buist, G.A. Chase, J.G. Donahue, M.J. Goodman, J.H. Gurwitz, A.Z. LaCroix, R. Platt, Inhibitors of hydroxymethylglutaryl-coenzyme A reductase and risk of fracture among older women, Lancet 355 (2000) 2185–2188.
[6] G. Lupattelli, A.M. Scarponi, G. Vaudo, D. Siepi, A.R. Roscini, F. Gemelli, M. Pirro, R.A. Latini, H. Sinzinger, S. Marchesi, E. Mannarino, Simvastatin increases bone mineral density in hypercholesterolemic postmenopausal women, Metabolism 53 (2004) 744–748.
[7] V. Bieghs, P.J. Van Gorp, K. Wouters, T. Hendrikx, M.J. Gijbels, M. van Bilsen, J. Bakker, C.J. Binder, D. Lutjohann, B. Staels, M.H. Hofker, R. Shiri-Sverdlov, LDL receptor knock-out mice are a physiological model particularly vulnerable to study the onset of inflammation in non-alcoholic fatty liver disease, PLoS One 7 (2012), e30668.
[8] M.L. Bonfleur, E.C. Vanzela, R.A. Ribeiro, D.G. de Gabriel, C.P. de Franca Carvalho, C.B. Collares-Buzato, E.M. Carneiro, A.C. Boschero, H.C. de Oliveira, Primary hypercholesterolaemia impairs glucose homeostasis and insulin secretion in low-density lipoprotein receptor knockout mice independently of high-fat diet and obesity, Biochim. Biophys. Acta 2010 (1801) 183–190.
[9] E.A. Soares, W.R. Nakagaki, J.A. Garcia, J.A. Camilli, Effect of hyperlipidemia on femoral biomechanics and morphology in low-density lipoprotein receptor gene knockout mice, J. Bone Miner. Metab. 30 (2012) 419–425.
[10] G.W. Go, Low-density lipoprotein receptor-related protein 6 (LRP6) is a novel nutritional therapeutic target for hyperlipidemia, non-alcoholic fatty liver disease, and atherosclerosis, Nutrients 7 (2015) 4453–4464.
[11] A. Saarinen, T. Saukkonen, T. Kivela, U. Lahtinen, C. Laine, M. Somer, S. Toiviainen-Salo, W.G. Cole, A.E. Lehesjoki, O. Makitie, Low density lipoprotein receptor-related protein 5 (LRP5) mutations and osteoporosis, impaired glucose metabolism and hypercholesterolaemia, Clin. Endocrinol. 72 (2010) 481–488.
[12] S.L. Holmen, T.A. Giambernardi, C.R. Zylstra, B.D. Buckner-Berghuis, J.H. Resau, J.F. Hess, V. Glatt, M.L. Bouxsein, M. Ai, M.L. Warman, B.O. Williams, Decreased BMD and limb deformities in mice carrying mutations in both Lrp5 and Lrp6, J. Bone Miner. Res. 19 (2004) 2033–2040.
[13] R. Levasseur, D. Lacombe, M.C. de Vernejoul, LRP5 mutations in osteoporosis-pseudoglioma syndrome and high-bone-mass disorders, Joint Bone Spine 72 (2005) 207–214.
[14] E.J. Samelson, L.A. Cupples, M.T. Hannan, P.W. Wilson, S.A. Williams, V. Vaccarino, Y. Zhang, D.P. Kiel, Long-term effects of serum cholesterol on bone mineral density in women and men: the Framingham Osteoporosis Study, Bone 34 (2004) 557–561.
[15] D.H. Solomon, J. Avorn, C.F. Canning, P.S. Wang, Lipid levels and bone mineral density, Am. J. Med. 118 (2005) 1414.
[16] M. Okayasu, M. Nakayachi, C. Hayashida, J. Ito, T. Kaneda, M. Masuhara, N. Suda, T. Sato, Y. Hakeda, Low-density lipoprotein receptor deficiency causes impaired osteoclastogenesis and increased bone mass in mice because of defect in osteoclastic cell-cell fusion, J. Biol. Chem. 287 (2012) 19229–19241.
[17] J.J. Cao, B.R. Gregoire, H. Gao, High-fat diet decreases cancellous bone mass but has no effect on cortical bone mass in the tibia in mice, Bone 44 (2009) 1097–1104.
[18] J.J. Cao, L. Sun, H. Gao, Diet-induced obesity alters bone remodeling leading to decreased femoral trabecular bone mass in mice, Ann. N. Y. Acad. Sci. 1192 (2010) 292–297.
[19] L. Shu, E. Beier, T. Sheu, H. Zhang, M.J. Zuscik, E.J. Puzas, B.F. Boyce, R.A. Mooney, L. Xing, High-fat diet causes bone loss in young mice by promoting osteoclastogenesis

through alteration of the bone marrow environment, Calcif. Tissue Int. 96 (2015) 313–323.
[20] J.M. Patsch, F.W. Kiefer, P. Varga, P. Pail, M. Rauner, D. Stupphann, H. Resch, D. Moser, P.K. Zysset, T.M. Stulnig, P. Pietschmann, Increased bone resorption and impaired bone microarchitecture in short-term and extended high-fat diet-induced obesity, Metabolism 60 (2011) 243–249.
[21] F. Parhami, Y. Tintut, W.G. Beamer, N. Gharavi, W. Goodman, L.L. Demer, Atherogenic high-fat diet reduces bone mineralization in mice, J. Bone Miner. Res. 16 (2001) 182–188.
[22] F. Pirih, J. Lu, F. Ye, O. Bezouglaia, E. Atti, M.G. Ascenzi, S. Tetradis, L. Demer, T. Aghaloo, Y. Tintut, Adverse effects of hyperlipidemia on bone regeneration and strength, J. Bone Miner. Res. 27 (2012) 309–318.
[23] N.K. Lee, H. Sowa, E. Hinoi, M. Ferron, J.D. Ahn, C. Confavreux, R. Dacquin, P.J. Mee, M.D. McKee, D.Y. Jung, Z. Zhang, J.K. Kim, F. Mauvais-Jarvis, P. Ducy, G. Karsenty, Endocrine regulation of energy metabolism by the skeleton, Cell 130 (2007) 456–469.
[24] P. Ducy, M. Amling, S. Takeda, M. Priemel, A.F. Schilling, F.T. Beil, J. Shen, C. Vinson, J.M. Rueger, G. Karsenty, Leptin inhibits bone formation through a hypothalamic relay: a central control of bone mass, Cell 100 (2000) 197–207.
[25] X.X. Chen, T. Yang, Roles of leptin in bone metabolism and bone diseases, J. Bone Miner. Metab. 33 (2015) 474–485.
[26] G.M. Kowalski, A.L. Carey, A. Selathurai, B.A. Kingwell, C.R. Bruce, Plasma sphingosine-1-phosphate is elevated in obesity, PLoS One 8 (2013), e72449.
[27] F. Samad, K.D. Hester, G. Yang, Y.A. Hannun, J. Bielawski, Altered adipose and plasma sphingolipid metabolism in obesity: a potential mechanism for cardiovascular and metabolic risk, Diabetes 55 (2006) 2579–2587.
[28] B.T. Bikman, A role for sphingolipids in the pathophysiology of obesity-induced inflammation, Cell. Mol. Life Sci. 69 (2012) 2135–2146.
[29] M. Ishii, J.G. Egen, F. Klauschen, M. Meier-Schellersheim, Y. Saeki, J. Vacher, R.L. Proia, R.N. Germain, Sphingosine-1-phosphate mobilizes osteoclast precursors and regulates bone homeostasis, Nature 458 (2009) 524–528.
[30] M. Ishii, J. Kikuta, Y. Shimazu, M. Meier-Schellersheim, R.N. Germain, Chemorepulsion by blood S1P regulates osteoclast precursor mobilization and bone remodeling in vivo, J. Exp. Med. 207 (2010) 2793–2798.
[31] M. Zhou, J. Ma, S. Chen, X. Chen, X. Yu, MicroRNA-17-92 cluster regulates osteoblast proliferation and differentiation, Endocrine (2013).
[32] T. Xia, Y. Liang, J. Ma, M. Li, M. Gong, X. Yu, Loss-of-function of SHARPIN causes an osteopenic phenotype in mice, Endocrine 39 (2011) 104–112.
[33] M. Zhou, J. Ma, S. Chen, X. Chen, X. Yu, MicroRNA-17-92 cluster regulates osteoblast proliferation and differentiation, Endocrine 45 (2014) 302–310.
[34] X. Yu, O.A. Ibrahimi, R. Goetz, F. Zhang, S.I. Davis, H.J. Garringer, R.J. Linhardt, D.M. Ornitz, M. Mohammadi, K.E. White, Analysis of the biochemical mechanisms for the endocrine actions of fibroblast growth factor-23, Endocrinology 146 (2005) 4647–4656.
[35] Y. Li, C. Ge, R.T. Franceschi, MAP kinase-dependent RUNX2 phosphorylation is necessary for epigenetic modification of chromatin during osteoblast differentiation, J. Cell. Physiol. (2016).
[36] M. Asagiri, H. Takayanagi, The molecular understanding of osteoclast differentiation, Bone 40 (2007) 251–264.
[37] J. Kikuta, M. Ishii, Osteoclast migration, differentiation and function: novel therapeutic targets for rheumatic diseases, Rheumatology (Oxford) 52 (2013) 226–234.
[38] Y. Tintut, S. Morony, L.L. Demer, Hyperlipidemia promotes osteoclastic potential of bone marrow cells ex vivo, Arterioscler. Thromb. Vasc. Biol. 24 (2004) e6–10.
[39] J. Cao, G. Ou, N. Yang, K. Ding, B.E. Kream, M.W. Hamrick, C.M. Isales, X.M. Shi, Impact of targeted PPARgamma disruption on bone remodeling, Mol. Cell. Endocrinol. 410 (2015) 27–34.
[40] M. Kawai, C.J. Rosen, PPARgamma: a circadian transcription factor in adipogenesis and osteogenesis, Nat. Rev. Endocrinol. 6 (2010) 629–636.
[41] D.A. Cook, S.W. Fellgett, M.E. Pownall, P.J. O'Shea, P.G. Genever, Wnt-dependent osteogenic commitment of bone marrow stromal cells using a novel GSK3beta inhibitor, Stem Cell Res. 12 (2014) 415–427.
[42] Z.E. Floyd, J.M. Stephens, Controlling a master switch of adipocyte development and insulin sensitivity: covalent modifications of PPARgamma, Biochim. Biophys. Acta 2012 (1822) 1090–1095.
[43] Z. Jin, W. Wei, H. Huynh, Y. Wan, HDAC9 inhibits osteoclastogenesis via mutual suppression of PPARgamma/RANKL signaling, Mol. Endocrinol. 29 (2015) 730–738.
[44] Y. Wan, L.W. Chong, R.M. Evans, PPAR-gamma regulates osteoclastogenesis in mice, Nat. Med. 13 (2007) 1496–1503.
[45] T. Fukunaga, W. Zou, N. Rohatgi, J.R. Colca, S.L. Teitelbaum, An insulin-sensitizing thiazolidinedione, which minimally activates PPARgamma, does not cause bone loss, J. Bone Miner. Res. 30 (2015) 481–488.
[46] S. Choi, A.J. Snider, Sphingolipids in high fat diet and obesity-related diseases, Mediat. Inflamm. 2015 (2015) 520618.
[47] T. Braun, G. Schett, Pathways for bone loss in inflammatory disease, Curr. Osteoporos. Rep. 10 (2012) 101–108.
[48] B.J. Kim, J.M. Koh, S.Y. Lee, Y.S. Lee, S.H. Lee, K.H. Lim, E.H. Cho, S.W. Kim, T.H. Kim, S.Y. Kim, G.S. Kim, Plasma sphingosine 1-phosphate levels and the risk of vertebral fracture in postmenopausal women, J. Clin. Endocrinol. Metab. 97 (2012) 3807–3814.
[49] E. Neumann, S. Junker, G. Schett, K. Frommer, U. Muller-Ladner, Adipokines in bone disease, Nat. Rev. Rheumatol. 12 (2016) 296–302.
[50] M. Scotece, J. Conde, K. Vuolteenaho, A. Koskinen, V. Lopez, J. Gomez-Reino, F. Lago, E. Moilanen, O. Gualillo, Adipokines as drug targets in joint and bone disease, Drug Discov. Today 19 (2014) 241–258.
[51] X. Chen, H.M. Tian, F.X. Pei, X.J. Yu, Bone functions as a novel endocrine organ in energy metabolism, Chin. Med. J. 125 (2012) 4117–4121.
[52] V. Mpalaris, P. Anagnostis, A.D. Anastasilakis, D.G. Goulis, A. Doumas, I. Iakovou, Serum leptin, adiponectin and ghrelin concentrations in post-menopausal women: is there an association with bone mineral density? Maturitas 88 (2016) 32–36.
[53] F. Elefteriou, S. Takeda, K. Ebihara, J. Magre, N. Patano, C.A. Kim, Y. Ogawa, X. Liu, S.M. Ware, W.J. Craigen, J.J. Robert, C. Vinson, K. Nakao, J. Capeau, G. Karsenty, Serum leptin level is a regulator of bone mass, Proc. Natl. Acad. Sci. U. S. A. 101 (2004) 3258–3263.